Editors' Suggestion | Featured in Physics

Preferred Spin Excitations in the Bilayer Iron-Based Superconductor $CaK(Fe_{0.96}Ni_{0.04})_4As_4$ with Spin-Vortex Crystal Order

Chang Liu,[1,2] Philippe Bourges,[3,*] Yvan Sidis,[3] Tao Xie,[4] Guanghong He,[5] Frédéric Bourdarot,[6] Sergey Danilkin,[7] Haranath Ghosh,[8,9] Soumyadeep Ghosh,[8,9] Xiaoyan Ma,[1,2] Shiliang Li,[1,2,10] Yuan Li,[5,11,†] and Huiqian Luo[1,10,‡]

[1]*Beijing National Laboratory for Condensed Matter Physics, Institute of Physics, Chinese Academy of Sciences, Beijing 100190, China*
[2]*School of Physical Sciences, University of Chinese Academy of Sciences, Beijing 100190, China*
[3]*Laboratoire Léon Brillouin, CEA-CNRS, Université Paris-Saclay, CEA Saclay, 91191 Gif-sur-Yvette, France*
[4]*Neutron Scattering Division, Oak Ridge National Laboratory, Oak Ridge, Tennessee 37831, USA*
[5]*International Center for Quantum Materials, School of Physics, Peking University, Beijing 100871, China*
[6]*Université Grenoble Alpes, CEA, INAC, MEM MDN, F-38000 Grenoble, France*
[7]*Australian Centre for Neutron Scattering, Australian Nuclear Science and Technology Organization, Lucas Heights NSW-2234, Australia*
[8]*Human Resources Development Section, Raja Ramanna Centre for Advanced Technology, Indore 452013, India*
[9]*Homi Bhabha National Institute, BARC training school complex 2nd floor, Anushakti Nagar, Mumbai 400094, India*
[10]*Songshan Lake Materials Laboratory, Dongguan, Guangdong 523808, China*
[11]*Collaborative Innovation Center of Quantum Matter, Beijing 100871, China*

(Received 10 January 2022; accepted 23 February 2022; published 31 March 2022)

Spin-orbit coupling (SOC) is a key to understand the magnetically driven superconductivity in iron-based superconductors, where both local and itinerant electrons are present and the orbital angular momentum is not completely quenched. Here, we report a neutron scattering study on the bilayer compound $CaK(Fe_{0.96}Ni_{0.04})_4As_4$ with superconductivity coexisting with a noncollinear spin-vortex crystal magnetic order that preserves the tetragonal symmetry of the Fe-Fe plane. In the superconducting state, two spin resonance modes with odd and even L symmetries due to the bilayer coupling are found similar to the undoped compound $CaKFe_4As_4$ but at lower energies. Polarization analysis reveals that the odd mode is c-axis polarized, and the low-energy spin anisotropy can persist to the paramagnetic phase at high temperature, which closely resembles other systems with in-plane collinear and c-axis biaxial magnetic orders. These results provide the missing piece of the puzzle on the SOC effect in iron-pnictide superconductors, and also establish a common picture of c-axis preferred magnetic excitations below T_c regardless of the details of magnetic pattern or lattice symmetry.

DOI: 10.1103/PhysRevLett.128.137003

The iron-based superconductivity emerges from a magnetic Hund's metal with strong interplay between the itinerant charge carriers on the Fermi surfaces and the local spins on Fe atoms [1–4]. In general, the magnetic orders in iron pnictide superconductors can be described by a unified function of the spatial variation of the Fe moments $\mathbf{m}$ at position $\mathbf{R}$: $\mathbf{m}(\mathbf{R}) = \mathbf{M_1}\cos(\mathbf{Q_1}\cdot\mathbf{R}) + \mathbf{M_2}\cos(\mathbf{Q_2}\cdot\mathbf{R})$, where $\mathbf{M_{1,2}}$ are two magnetic order parameters associated with two orthogonal wave vectors $\mathbf{Q_{1,2}}$ [e.g., $\mathbf{Q_1} = (\pi, 0)$ and $\mathbf{Q_2} = (0, \pi)$] [5]. There are three confirmed magnetic patterns listed below [6]: (1) the collinear stripe-type order with in-plane moments given by $\mathbf{M_1} \neq 0$ and $\mathbf{M_2} = 0$, the so-called stripe spin-density wave (SSDW) [7,8]; (2) the collinear biaxial order with c-axis polarized moments given by $|\mathbf{M_1}| = |\mathbf{M_2}| \neq 0$ and $\mathbf{M_1} \| \mathbf{M_2}$, the so-called charge-spin-density wave (CSDW) [9,10]; (3) the noncollinear, coplanar order with in-plane moments given by $|\mathbf{M_1}| = |\mathbf{M_2}| \neq 0$ and $\mathbf{M_1} \perp \mathbf{M_2}$, the so-called spin-vortex crystal (SVC) phase [11,12]. While the latter two cases preserve the tetragonal symmetry of the lattice, the presence of the first one has to break the C_4 rotational symmetry by a tetragonal-to-orthorhombic structural transition, leading to an Ising-nematic electronic phase prior to the magnetic ordering [13,14].

All three magnetic phases are proximate to each other in the mean-field phase diagram within the Ginzburg-Landau framework [Fig. 1(a)], where the magnetic ground state is determined by the signs of Landau parameters (g, w, and η) and the form of spin-orbit coupling (SOC) in actual materials [5,15]. The coupling between local spins and five $3d$ Fe orbitals is essential not only to stabilize the static magnetic order but also to modify the dynamic spin fluctuations [16,17]. Since the spin fluctuations most likely promote the sign-reversed superconducting pairing between the hole and electron Fermi pockets (the so-called $s^{\pm}$ pairing) [18,19], the SOC will certainly show influence on the formation of superconductivity. Such an effect can be traced in the anisotropy of the neutron spin resonant

mode around the ordered wave vector **Q**, which is usually interpreted as an excitonic bound state from the renormalized spin excitations in the superconducting state [20–25]. Interestingly, it seems that the spin resonance in many iron pnictide superconductors is preferentially polarized along c axis, not only for those compounds with in-plane SSDW order [e.g., $BaFe_{2-x}(Ni, Co)_xAs_2$, $BaFe_2(As_{1-x}P_x)_2$, and $NaFe_{1-x}Co_xAs$] [26–33], but also for the underdoped $(Ba, Sr)_{1-x}Na_xFe_2As_2$ with c-axis oriented CSDW [34,35] and the optimally doped $Ba_{1-x}K_xFe_2As_2$ [36–38]. This mode seems to be fully c-axis polarized in paramagnetic FeSe [39]. Whether the resonant mode in iron-based superconductors is universally c-axis polarized needs to be finally investigated in the compounds with coplanar SVC order.

Here in this Letter, we address the issue of spin anisotropies in the bilayer iron-based superconductor $CaK(Fe_{1-x}Ni_x)_4As_4$ with coexisting superconductivity and SVC magnetic order. Our unpolarized inelastic neutron scattering measurements reveal two spin resonance modes at about 7 and 15 meV with odd and even L symmetries, respectively. Polarization analysis suggests that the odd mode is highly anisotropic, manifested by a strong c-axis component and two weakly anisotropic in-plane components ($M_c \gg M_b > M_a$). The c-axis preferred spin excitations already show up in the SVC phase and even continue to the paramagnetic phase until the spin anisotropy finally disappears at about $T = 100$ K, which probably is a consequence from the SOC associated with the spontaneously broken electronic symmetries in SVC and its vestigial states. These results suggest a common feature of c-axis preferred spin excitations below T_c regardless of their magnetic patterns or lattice symmetries in iron pnictide superconductors.

The $CaK(Fe_{1-x}Ni_x)_4As_4$ system belongs to a 1144-type iron-based superconductor, where the stoichiometric compound $CaKFe_4As_4$ already shows a superconductivity below $T_c = 35$ K without any magnetic order [40,41]. The Ni doping will suppress the superconducting transition and induce a SVC order when $x \geq 0.02$ [Fig. 1(b)] [11,12]. Its lattice retains the tetragonal symmetry against the chemical doping and temperature, but the translational symmetry along the c axis is broken due to the two inequivalent As sites below and above the Fe-Fe plane [Fig. 1(c)] [42,43]. As the moments $\mathbf{M_{1,2}}$ are mutually perpendicular to preserve the tetragonal lattice symmetry, the continuous rotational symmetry is broken from $O(3)$ to $O(2)$ for the magnetism [Fig. 1(e)]. Thus a unique SOC is theoretically proposed in the form of a vector chiral order parameter $\boldsymbol{\varphi} = 2\omega\langle \mathbf{M_1} \times \mathbf{M_2} \rangle$, giving a vestigial phase called spin-vorticity density wave (SVDW) [5,15,16,44]. In our previous neutron scattering measurements on $CaKFe_4As_4$, it is found that the spin resonance splits into two nondegenerate modes with odd or even L modulations induced by the broken translational symmetry along c axis

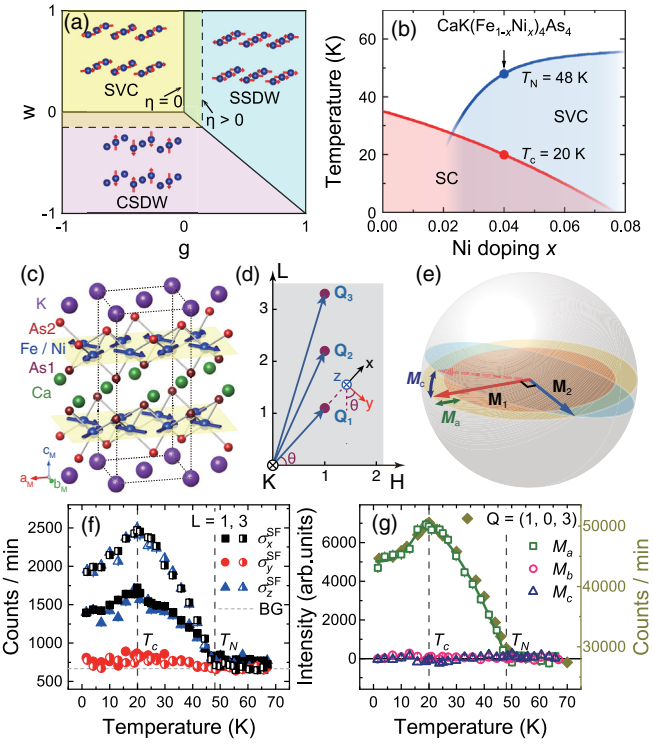

FIG. 1. (a) Mean-field phase diagram of the magnetic states in iron pnictides [15]. (b),(c) Phase diagram and SVC magnetic structure of $CaK(Fe_{1-x}Ni_x)_4As_4$ [11]. The arrow marks the doping in this study. (d) The scattering plane and the definition of spin-polarization directions in reciprocal space. (e) Schematic picture of the fluctuating moments under SVC order. Assuming $\mathbf{M_2}$ is fixed, $\mathbf{M_1}$ is allowed to fluctuate either transverse out of plane (M_c) or longitudinal in plane (M_a). (f) Magnetic order parameter at $Q = (1, 0, 1)$ and $(1, 0, 3)$ measured by polarized elastic neutron scattering. (g) Three components of static moments (open) in comparison with the unpolarized results (solid).

[45], and the low-energy odd modes are indeed c-axis polarized [46]. Here, we focus on the Ni doped compound $CaK(Fe_{0.96}Ni_{0.04})_4As_4$ with coexisting superconductivity ($T_c = 20.1 \pm 0.9$ K) and SVC order ($T_N = 48.1 \pm 2.1$ K) [47]. The crystals were grown by the self-flux method with less than 5% inhomogeneity of Ni doping, and coaligned on the scattering plane $[H,0,0] \times [0,0,L]$ by hydrogen-free glue [45–47]. The magnetic unit cell ($a_M = b_M = 5.398$ Å, $c = 12.616$ Å) was used to define the wave vector **Q** at (q_x, q_y, q_z) by $(H, K, L) = (q_x a_M/2\pi, q_y b_M/2\pi, q_z c/2\pi)$ in reciprocal lattice units (r.l.u.) [45]. Unpolarized neutron scattering experiments were carried out using the Taipan spectrometer at ACNS, ANSTO, Australia, and polarized neutron scattering experiments were performed at the CEA-CRG IN22 spectrometer in ILL, Grenoble, France, using the CryoPAD system and Heusler monochromator and analyzer [64]. The neutron-polarization directions were defined as x, y, z, with x parallel to the momentum transfer **Q**, and y and z perpendicular to **Q** [Fig. 1(d)]. We focused on the spin-flip (SF) channels both before and after the

sample given by three cross sections: σ_x^{SF}, σ_y^{SF}, and σ_z^{SF}, which is only sensitive to the magnetic excitations or moments that are perpendicular to $\mathbf{Q}$ [26–38]. The measured intensity is related to the magnetic form factor $F(Q)$ [or structural factor $f_M(Q)$] and orientation of ordered moments, it can be also affected by the instrument resolution and higher-harmonic scattering from the monochromator [47,65,66]. After considering the geometries of lattice and polarization at two unparallel but equivalent wave vectors, we can separate all three magnetic excitation components: M_a, M_b, and M_c along the lattice axes a_M, b_M, and c, respectively [23,29,32,38,46,47]. The background from the leakage of the non-spin-flipping channel and the incoherent scattering can also be estimated [46,47].

We first present the elastic neutron scattering results to confirm the SVC order. The SVC phase is antiferromagnetically ordered along the c axis with magnetic peaks at $Q = (1, 0, L)$ $(L = 0, \pm 1, \pm 2, \pm 3, \pm 4, \ldots)$, where the peaks at odd L's are much stronger than those at even L's [12]. Figure 1(f) shows the temperature dependence of magnetic peak intensity (magnetic order parameter) at $Q = (1, 0, 1)$ and (1, 0, 3) for all three SF channels. The magnetic peak intensities concentrate in σ_x^{SF} and σ_z^{SF} channels, leaving a nearly flat background in σ_y^{SF}, where the competition between the magnetism and superconductivity suppresses the intensity below $T_c = 20.1$ K. We have estimated all the three components of the static moments M_a, M_b, and M_c as shown in Fig. 1(g). Only the in-plane component M_a has nonzero value and shows the same temperature dependence as unpolarized results. Therefore, the ordered moments indeed lay within the ab plane where the moments $\mathbf{M_1}$ are antiferromagnetic along $\mathbf{Q_1} = (\pi, 0)$, consistent with the geometry of coplanar SVC order. The other ordered wave vector $\mathbf{Q_2} = (0, \pi)$ of $\mathbf{M_2}$ cannot be reached in this scattering plane.

The inelastic neutron scattering results with unpolarized beam are presented in Fig. 2. After subtracting the intensities in the normal state (25 K) from the low temperature data in the superconducting state (2 K), two spin resonant modes at $Q = (1, 0, 3)$ and (1, 0, 2) are immediately observable. While the mode at $L = 3$ is centered around 7 meV, the mode at $L = 2$ is around 15 meV, and both of them are broad in energy distribution [Fig. 2(a)]. The L modulation of each mode follows odd symmetry $\sim|F(Q)|^2\sin^2(z\pi L)$ or even symmetry $\sim|F(Q)|^2\cos^2(z\pi L)$ with respect to the reduced distance $zc = 5.849$ Å $(z \approx 0.464)$ within the Fe-As bilayer unit [Fig. 2(b)]. Such results are attributed to the nondegenerate spin excitations induced by the bilayer magnetic coupling, which were previously observed in the undoped compound $CaKFe_4As_4$ [45]. By tracking the temperature dependence of intensities at $E = 7$ meV, $Q = (1, 0, 3)$, and $E = 17$ meV, $Q = (1, 0, 2)$, the order-parameter-like intensity gains are clearly observed below T_c for both modes [Fig. 2(c)]. We also compare the intensity under the

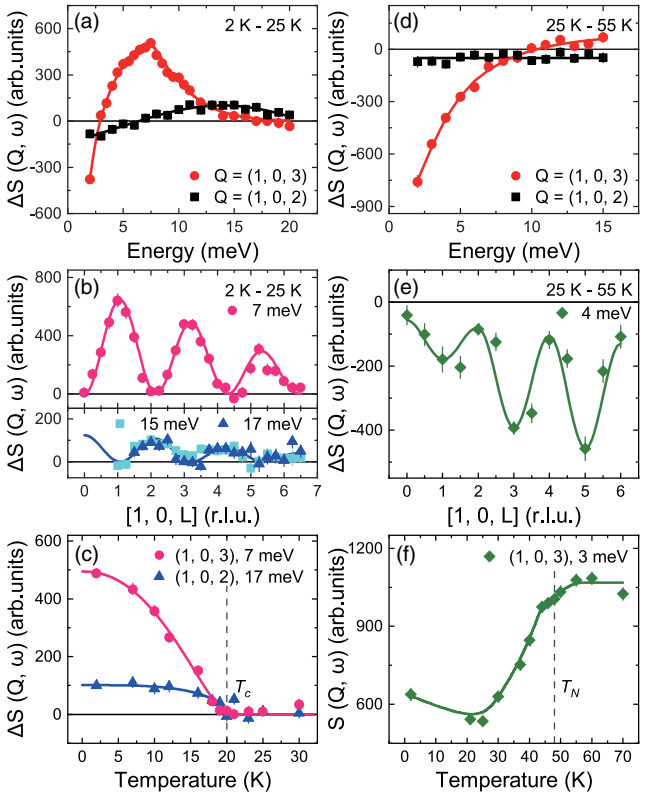

FIG. 2. Unpolarized neutron scattering results on the low-energy spin excitations in $CaK(Fe_{0.96}Ni_{0.04})_4As_4$. (a) The odd and even spin resonant modes at $Q = (1, 0, 3)$ and (1, 0, 2), respectively. (b) L modulations of two spin resonant modes at $E = 7$, 15, and 17 meV. (c) Temperature dependence of the spin resonant intensity at $E = 7$ and 17 meV. (d) Partially gapped spin excitations at $Q = (1, 0, 3)$ in comparison with those at $Q = (1, 0, 2)$. (e) L modulations of the spin gap at $E = 4$ meV. (f) Temperature dependence of the intensity at $E = 3$ meV and $Q = (1, 0, 3)$. All solid lines are guides to the eyes.

SVC ordered state at $T = 25$ K and the paramagnetic state at $T = 55$ K. It seems that the spin excitations are partially suppressed below 10 meV, giving negative values for 25–55 K data with strong odd L modulations [Figs. 2(d) and 2(e)]. After considering the effect from the Bose factor, the spin gap energy is determined to be around 6 meV [47]. It exhibits a transitionlike behavior across T_N [Fig. 2(f)]. Such spin-gapped behavior may be related to some soft excitations in the paramagnetic state, which is cleared up below T_N with spectral weight condensed into the SVC Bragg peaks, and thus more obvious at $L =$ odd than $L =$ even [12]. In the SSDW systems, the spin gap is also three dimensional due to the interlayer exchange coupling J_c [13,67].

Having established the L dependence of spin excitations at different temperatures, we then perform polarization analysis on the anisotropy of low-energy excitations in spin space. The raw data of the energy and temperature dependence of σ_x^{SF}, σ_y^{SF}, and σ_z^{SF} are presented in the Supplemental Material [47], the deduced dynamic spin

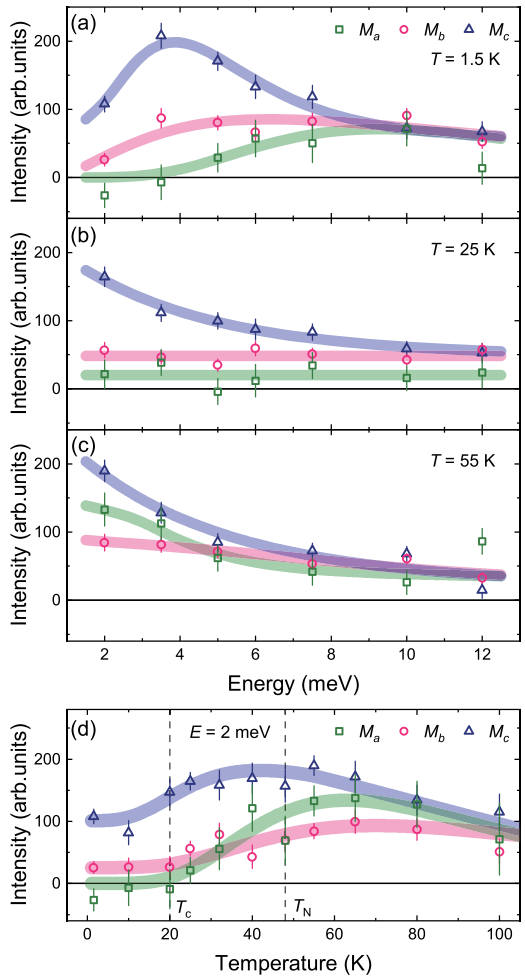

FIG. 3. Polarization analysis on the low-energy spin excitations in $CaK(Fe_{0.96}Ni_{0.04})_4As_4$. (a)–(c) Energy dependence of M_a, M_b, and M_c at $T = 1.5$, 25, and 55 K deduced from three SF cross sections: σ_x^{SF}, σ_y^{SF}, and σ_z^{SF}. (d) Temperature dependence of M_a, M_b, and M_c at 2 meV. All bold lines are guides to the eyes.

components M_a, M_b, and M_c, are shown in Fig. 3. For the odd mode in the superconducting state, there is a c-axis polarized component that peaked around $E = 4$ meV, and the in-plane excitations are also weakly anisotropic below $E = 10$ meV. At the intermediate temperature $T = 25$ K, the spin resonance disappears, but the spin anisotropy still persists. When further warming up into the paramagnetic state, where the spin gap closes thus the low-energy spin excitations increase, the spin anisotropy only exists below 5 meV. Figure 3(d) shows M_a, M_b, and M_c as a function of temperature at the lowest energy we can approach ($E = 2$ meV). It is evident that the c-axis component M_c is always stronger than the in-plane components M_a and M_b, and the spin anisotropy can persist up to a very high temperature of about 100 K, about twice of T_N. Such behavior is reminiscent of the results in $BaFe_{2-x}Ni_xAs_2$, $Ba_{1-x}K_xFe_2As_2$, and $NaFe_{1-x}Co_xAs$, where the low-energy spin anisotropy can survive well above T_N in the paramagnetic state [29,31,38].

The confirmation of c-axis dominated spin excitations in this Letter establishes a universal feature in iron pnictides that the pairing of itinerant electrons prefers to be assisted by c-axis spin fluctuations, no matter that the magnetic pattern is an in-plane collinear SSDW, c-axis biaxial CSDW, or coplanar SVC. This could naturally explain the positive correlation between the maximum energies of SOC induced spin anisotropy and T_c [38,46], if the low-energy spin fluctuations indeed act as the bosonic "pairing glue" in the formation of unconventional superconductivity. The spin resonance, as a bound state of collective excitations from gapped charge carriers near the Fermi level, is formed by the spectral weight transfer from low energy to resonant energy of the spin excitations which are already present in the normal state above T_c. In the SSDW phase, the ordered moments are along the a axis and much easier to rotate perpendicularly to the FeAs plane than within the plane, resulting in prominent spin fluctuations along c axis (M_c) in the antiferromagnetic state [68,69]. Thus M_c also takes the leading contribution in the superconducting state under the SOC between itinerant electrons and local moments [29,31]. The in-plane spin anisotropy depends on the nematic susceptibility and the gapped intensities due to magnetic ordering [29,32,35]. In the CSDW phase with c-axis spin reorientation, although the magnetic order already suppresses most of the longitudinal excitations (M_c) above T_c, it seems that the itinerant electrons still keep the c-axis "memory" in the superconducting state [34,35]. Here the case of the SVC phase is similar to that in the SSDW phase, the in-plane longitudinal mode M_a is suppressed below T_N due to the magnetic ordering [Figs. 3(b) and 3(c)]. On the other hand, the c-axis component (M_c) is well preserved, leaving enough spectral weight to form the spin resonance below T_c [Fig. 3(a)]. The universality of the c-axis preferred spin resonance supports the orbital-selective pairing in iron-pnictide superconductors [62,70,71]. The Cooper pairs might be favored by particular orbital orders, which are robustly coupled to the local spins of Fe in most systems even at high temperatures far above T_c.

Finally, we notice that the in-plane spin excitations seem to be weakly anisotropic, such effect probably relates to the electronic nematicity involved with in-plane orbital ordering. Although the nematic order is absent in the tetragonal 1144 system, the nematic fluctuations are probed in transport measurements [15,72], and possible orbital orders are proposed in the band calculations [47,62]. Moreover, the anisotropy between M_a and M_b can be effectively considered as the total moment on Fe sites rotating off the diagonal direction, leading to either clockwise or counterclockwise movement of the SVC-type plaquette described by the chiral order parameter of the SVDW ($\boldsymbol{\varphi}$) [5]. This SVDW phase is critical to affect the nematic fluctuations, as it bridges two nearly degenerate phases (SVC and SSDW) in the mean-field phase diagram, where the parameter η in

Fig. 1(a) can be viewed as a conjugate field to $\boldsymbol{\varphi}$ [15,73]. By tuning η from zero to finite, the degenerated region between the SVC and SSDW phases (or between the SVC and CSDW phases) increases, then the magnetic phase may easily transform to another under the assistance of SOC [15]. This explains the competition between SSDW and CSDW in the hole-underdoped compounds [9,10] as well as the additional c-axis moments induced by uniaxial pressure in the parent compound $BaFe_2As_2$ [74].

In summary, we have revealed the L dependence and anisotropy of the low-energy spin excitations in the 1144-type $CaK(Fe_{0.96}Ni_{0.04})_4As_4$ with superconductivity below $T_c = 20.1$ K and a SVC order below $T_N = 48.1$ K under the tetragonal lattice symmetry. The bilayer coupling induced odd and even L modulations of the spin resonance are observed around 7 and 15 meV, respectively. The odd mode is highly anisotropic with c-axis preferred magnetic excitations, and the low-energy spin anisotropy persists up to a high temperature of about $T = 100$ K, much similar to those cases with in-plane collinear or c-axis biaxial magnetic order. These results suggest that the c-axis magnetic excitations are universally preferred by the presumably orbital-selective superconducting pairing. Meanwhile, the form of magnetic order depends on material-specific symmetry characteristics in addition to SOC, leading to a rich variety of interplay between superconductivity and magnetism in the Fe-based superconductors.

The raw data are available in Ref. [75].

This work is supported by the National Key R&D project of China (Grants No. 2020YFA0406003, No. 2018YFA0704200, No. 2018YFA0305602, and No. 2017YFA0302900), the National Natural Science Foundation of China (Grants No. 11822411, 11888101, No. 11874069, No. 11961160699, and No. 11674406), the Strategic Priority Research Program (B) of the CAS (Grants No. XDB25000000 and No. XDB07020300) and K. C. Wong Education Foundation (GJTD-2020-01). H. L. is grateful for the support from the Youth Innovation Promotion Association of CAS (Grant No. Y202001). Work at Oak Ridge National Laboratory was supported by the U.S. Department of Energy, Office of Science, Basic Energy Sciences, Materials Science and Engineering Division. S. G. acknowledges Homi Bhaba National Institute at Raja Ramanna Centre for Advanced Technology. P. B. and Y. S. acknowledge financial support from the Fédération Française de Diffusion Neutronique (2FDN).

*philippe.bourges@cea.fr
†yuan.li@pku.edu.cn
‡hqluo@iphy.ac.cn

[1] X. Chen, P. Dai, D. Feng, T. Xiang, and F. Zhang, Natl. Sci. Rev. **1**, 371 (2014).
[2] P. Dai, J. Hu, and E. Dagotto, Nat. Phys. **8**, 709 (2012).
[3] Q. Si, R. Yu, and E. Abrahams, Nat. Rev. Mater. **1**, 16017 (2016).
[4] A. Georges, L. de'Medici, and J. Mravlje, Annu. Rev. Condens. Matter Phys. **4**, 137 (2013).
[5] R. M. Fernandes, S. A. Kivelson, and E. Berg, Phys. Rev. B **93**, 014511 (2016).
[6] D. Gong and H. Luo, Acta Phys. Sin. **67**, 207407 (2018).
[7] J. Lorenzana, G. Seibold, C. Ortix, and M. Grilli, Phys. Rev. Lett. **101**, 186402 (2008).
[8] C. de la Cruz, Q. Huang, J. W. Lynn, J. Li, W. Ratcliff II, J. L. Zarestky, H. A. Mook, G. F. Chen, J. L. Luo, N. L. Wang, and P. Dai, Nature (London) **453**, 899 (2008).
[9] J. M. Allred, K. M. Taddei, D. E. Bugaris, M. J. Krogstad, S. H. Lapidus, D. Y. Chung, H. Claus, M. G. Kanatzidis, D. E. Brown, J. Kang, R. M. Fernandes, I. Eremin, S. Rosenkranz, O. Chmaissem, and R. Osborn, Nat. Phys. **12**, 493 (2016).
[10] A. E. Böhmer, F. Hardy, L. Wang, T. Wolf, P. Schweiss, and C. Meingast, Nat. Commun. **6**, 7911 (2015).
[11] W. R. Meier, Q.-P. Ding, A. Kreyssig, S. L. Bud'ko, A. Sapkota, K. Kothapalli, V. Borisov, R. Valentí, C. D. Batista, P. P. Orth, R. M. Fernandes, A. I. Goldman, Y. Furukawa, A. E. Böhmer, and P. C. Canfield, npj Quantum Mater. **3**, 5 (2018).
[12] A. Kreyssig, J. M. Wilde, A. E. Böhmer, W. Tian, W. R. Meier, B. Li, B. G. Ueland, M. Xu, S. L. Bud'ko, P. C. Canfield, R. J. McQueeney, and A. I. Goldman, Phys. Rev. B **97**, 224521 (2018).
[13] P. Dai, Rev. Mod. Phys. **87**, 855 (2015).
[14] X. Lu, J. T. Park, R. Zhang, H. Luo, Andriy. H. Nevidomskyy, Q. Si, and P. Dai, Science **345**, 657 (2014).
[15] A. E. Böhmer, F. Chen, W. R. Meier, M. Xu, G. Drachuck, M. Merz, P. W. Wiecki, S. L. Bud'ko, V. Borisov, R. Valentí, M. H. Christensen, R. M. Fernandes, C. Meingast, and P. C. Canfield, arXiv:2011.13207.
[16] M. H. Christensen, J. Kang, and R. M. Fernandes, Phys. Rev. B **100**, 014512 (2019).
[17] D. S. Inosov, C. R. Phys. **17**, 60 (2016).
[18] T. A. Maier, S. Graser, D. J. Scalapino, and P. Hirschfeld, Phys. Rev. B **79**, 134520 (2009).
[19] Z. Wang, H. Yang, D. Fang, B. Shen, Q.-H. Wang, L. Shan, C. Zhang, P. Dai, and H.-H. Wen, Nat. Phys. **9**, 42 (2013).
[20] M. Eschrig, Adv. Phys. **55**, 47 (2006).
[21] Y. Sidis, S. Pailhès, V. Hinkov, B. Fauqué, C. Ulrich, L. Capogna, A. Ivanov, L.-P. Regnault, B. Keimer, and P. Bourges, C. R. Phys. **8**, 745 (2007).
[22] A. D. Christianson, E. A. Goremychkin, R. Osborn, S. Rosenkranz, M. D. Lumsden, C. D. Malliakas, I. S. Todorov, H. Claus, D. Y. Chung, M. G. Kanatzidis, R. I. Bewley, and T. Guidi, Nature (London) **456**, 930 (2008).
[23] T. Xie, D. Gong, H. Ghosh, A. Ghosh, M. Soda, T. Masuda, S. Itoh, F. Bourdarot, L.-P. Regnault, S. Danilkin, S. Li, and H. Luo, Phys. Rev. Lett. **120**, 137001 (2018).
[24] W. Hong, L. Song, B. Liu, Z. Li, Z. Zeng, Y. Li, D. Wu, Q. Sui, T. Xie, S. Danilkin, H. Ghosh, A. Ghosh, J. Hu, L. Zhao, X. Zhou, X. Qiu, S. Li, and H. Luo, Phys. Rev. Lett. **125**, 117002 (2020).
[25] T. Xie, C. Liu, T. Fennell, U. Stuhr, S. Li, and H. Luo, Chin. Phys. B **30**, 127402 (2021).
[26] O. J. Lipscombe, L. W. Harriger, P. G. Freeman, M. Enderle, C. Zhang, M. Wang, T. Egami, J. Hu, T. Xiang, M. R. Norman, and P. Dai, Phys. Rev. B **82**, 064515 (2010).

[27] M. Liu, C. Lester, J. Kulda, X. Lu, H. Luo, M. Wang, S. M. Hayden, and P. Dai, Phys. Rev. B **85**, 214516 (2012).

[28] P. Steffens, C. H. Lee, N. Qureshi, K. Kihou, A. Iyo, H. Eisaki, and M. Braden, Phys. Rev. Lett. **110**, 137001 (2013).

[29] H. Luo, M. Wang, C. Zhang, X. Lu, L.-P. Regnault, R. Zhang, S. Li, J. Hu, and P. Dai, Phys. Rev. Lett. **111**, 107006 (2013).

[30] C. Zhang, Y. Song, L.-P. Regnault, Y. Su, M. Enderle, J. Kulda, G. Tan, Z. C. Sims, T. Egami, Q. Si, and P. Dai, Phys. Rev. B **90**, 140502(R) (2014).

[31] Y. Song, W. Wang, C. Zhang, Y. Gu, X. Lu, G. Tan, Y. Su, F. Bourdarot, A. D. Christianson, S. Li, and P. Dai, Phys. Rev. B **96**, 184512 (2017).

[32] D. Hu, W. Zhang, Y. Wei, B. Roessli, M. Skoulatos, L.-P. Regnault, G. Chen, Y. Song, H. Luo, S. Li, and P. Dai, Phys. Rev. B **96**, 180503(R) (2017).

[33] F. Waßer, C. H. Lee, K. Kihou, P. Steffens, K. Schmalzl, N. Qureshi, and M. Braden, Sci. Rep. **7**, 10307 (2017).

[34] J. Guo, L. Yue, K. Iida, K. Kamazawa, L. Chen, T. Han, Y. Zhang, and Y. Li, Phys. Rev. Lett. **122**, 017001 (2019).

[35] F. Waßer, J. T. Park, S. Aswartham, S. Wurmehl, Y. Sidis, P. Steffens, K. Schmalzl, B. Büchner, and M. Braden, npj Quantum Mater. **4**, 59 (2019).

[36] C. Zhang, M. Liu, Y. Su, L.-P. Regnault, M. Wang, G. Tan, Th. Brückel, T. Egami, and P. Dai, Phys. Rev. B **87**, 081101(R) (2013).

[37] N. Qureshi, C. H. Lee, K. Kihou, K. Schmalzl, P. Steffens, and M. Braden, Phys. Rev. B **90**, 100502(R) (2014).

[38] Y. Song, H. Man, R. Zhang, X. Lu, C. Zhang, M. Wang, G. Tan, L.-P. Regnault, Y. Su, J. Kang, R. M. Fernandes, and P. Dai, Phys. Rev. B **94**, 214516 (2016).

[39] M. Ma, P. Bourges, Y. Sidis, Y. Xu, S. Li, B. Hu, J. Li, F. Wang, and Y. Li, Phys. Rev. X **7**, 021025 (2017).

[40] A. Iyo, K. Kawashima, T. Kinjo, T. Nishio, S. Ishida, H. Fujihisa, Y. Gotoh, K. Kihou, H. Eisaki, and Y. Yoshida, J. Am. Chem. Soc. **138**, 3410 (2016).

[41] W. R. Meier, T. Kong, U. S. Kaluarachchi, V. Taufour, N. H. Jo, G. Drachuck, A. E. Böhmer, S. M. Saunders, A. Sapkota, A. Kreyssig, M. A. Tanatar, R. Prozorov, A. I. Goldman, F. F. Balakirev, A. Gurevich, S. L. Bud'ko, and P. C. Canfield, Phys. Rev. B **94**, 064501 (2016).

[42] W. R. Meier, T. Kong, S. L. Bud'ko, and P. C. Canfield, Phys. Rev. Mater. **1**, 013401 (2017).

[43] J. Cui, Q.-P. Ding, W. R. Meier, A. E. Böhmer, T. Kong, V. Borisov, Y. Lee, S. L. Bud'ko, R. Valentí, P. C. Canfield, and Y. Furukawa, Phys. Rev. B **96**, 104512 (2017).

[44] X. Wang and R. M. Fernandes, Phys. Rev. B **89**, 144502 (2014).

[45] T. Xie, Y. Wei, D. Gong, T. Fennell, U. Stuhr, R. Kajimoto, K. Ikeuchi, S. Li, J. Hu, and H. Luo, Phys. Rev. Lett. **120**, 267003 (2018).

[46] T. Xie, C. Liu, F. Bourdarot, L.-P. Regnault, S. Li, and H. Luo, Phys. Rev. Research **2**, 022018(R) (2020).

[47] See Supplemental Materials at http://link.aps.org/supplemental/10.1103/PhysRevLett.128.137003 for the sample information, polarized analysis and band calculations, which includes Refs. [48–63].

[48] Y. Chen, X. Lu, M. Wang, H. Luo, and S. Li, Supercond. Sci. Technol. **24**, 065004 (2011).

[49] H. Luo, R. Zhang, M. Laver, Z. Yamani, M. Wang, X. Lu, M. Wang, Y. Chen, S. Li, S. Chang, J. W. Lynn, and P. Dai, Phys. Rev. Lett. **108**, 247002 (2012).

[50] X. Lu, H. Gretarsson, R. Zhang, X. Liu, H. Luo, W. Tian, M. Laver, Z. Yamani, Y.-J. Kim, A. H. Nevidomskyy, Q. Si, and P. Dai, Phys. Rev. Lett. **110**, 257001 (2013).

[51] R. Zhang, D. Gong, X. Lu, S. Li, M. Laver, C. Niedermayer, S. Danilkin, G. Deng, P. Dai, and H. Luo, Phys. Rev. B **91**, 094506 (2015).

[52] T. Xie, D. Gong, W. Zhang, Y. Gu, Z. Huesges, D. Chen, Y. Liu, L. Hao, S. Meng, Z. Lu, S. Li, and H. Luo, Supercond. Sci. Technol. **30**, 095002 (2017).

[53] P. Giannozzi, O. Andreussi, T. Brumme *et al.*, J. Phys. Condens. Matter **29**, 465901 (2017).

[54] J. P. Perdew, K. Burke, and M. Ernzerhof, Phys. Rev. Lett. **77**, 3865 (1996).

[55] L. Bellaiche and D. Vanderbilt, Phys. Rev. B **61**, 7877 (2000).

[56] H. J. Monkhorst and J. D. Pack, Phys. Rev. B **13**, 5188 (1976).

[57] J. D. Pack and H. J. Monkhorst, Phys. Rev. B **16**, 1748 (1977).

[58] R. Fletcher, Comput. J. **13**, 317 (1970).

[59] D. Goldfarb, Math. Comp. **24**, 23 (1970).

[60] D. F. Shanno, Math. Comp. **24**, 647 (1970).

[61] M. Kawamura, Comput. Phys. Commun. **239**, 197 (2019).

[62] A. Ghosh, S. Sen, and H. Ghosh, Comput. Mater. Sci. **186**, 109991 (2021).

[63] F. Lochner, F. Ahn, T. Hickel, and I. Eremin, Phys. Rev. B **96**, 094521 (2017).

[64] E. Lelièvre-Berna, E. Bourgeat-Lami, P. Fouilloux *et al.*, Physica (Amsterdam) **356B**, 131 (2005).

[65] D. Gong, T. Xie, R. Zhang, J. Birk, C. Niedermayer, F. Han, S. H. Lapidus, P. Dai, S. Li, and H. Luo, Phys. Rev. B **98**, 014512 (2018).

[66] G. Shirane, S. M. Shapiro, and J. M. Tranquada, *Neutron Scattering with a Triple-Axis Spectrometer* (Cambridge University Press, Cambridge, England, 2004), pp. P23–P46, P170–P172 and pp. P117–P121.

[67] L. W. Harriger, A. Schneidewind, S. Li, J. Zhao, Z. Li, W. Lu, X. Dong, F. Zhou, Z. Zhao, J. Hu, and P. Dai, Phys. Rev. Lett. **103**, 087005 (2009).

[68] N. Qureshi, P. Steffens, S. Wurmehl, S. Aswartham, B. Büchner, and M. Braden, Phys. Rev. B **86**, 060410(R) (2012).

[69] C. Wang, R. Zhang, F. Wang, H. Luo, L. P. Regnault, P. Dai, and Y. Li, Phys. Rev. X **3**, 041036 (2013).

[70] R. Yu, H. Hu, E. M. Nica, J.-X. Zhu, and Q. Si, Front. Phys. **9**, 578347 (2021).

[71] L. Chen, T. T. Han, C. Cai, Z. G. Wang, Y. D. Wang, Z. M. Xin, and Y. Zhang, Phys. Rev. B **104**, L060502 (2021).

[72] W.-L. Zhang, W. R. Meier, T. Kong, P. C. Canfield, and G. Blumberg, Phys. Rev. B **98**, 140501(R) (2018).

[73] R. M. Fernandes and J. Schmalian, Supercond. Sci. Technol. **25**, 084005 (2012).

[74] P. Liu, M. L. Klemm, L. Tian, X. Lu, Y. Song, D. W. Tam, K. Schmalzl, J. T. Park, Y. Li, G. Tan, Y. Su, F. Bourdarot, Y. Zhao, J. W. Lynn, R. J. Birgeneau, and P. Dai, Nat. Commun. **11**, 5728 (2020).

[75] Y. Li, F. Bourdarot, P. Bourges, G. He, C. Liu, H. Luo, Y. Sidis, X. Wang, and T. Xie, Institut Laue-Langevin (ILL), 10.5291/ILL-DATA.CRG-2609 (2020).